RPN54

INTENSE BEAM GENERATION AT MEGAMPERE CURRENTS AND BEAM TRANSPORT IN PULSED EXTERNAL MAGNETIC FIELD CONFIGURATIONS

PIIR-27-71

by

B. Ecker, J. Benford, C. Stallings, S. Putnam, and P. Spence

May 1971

Presented at the
Eleventh Symposium on Electron, Ion, and
Laser Beam Technology
Boulder, Colorado
May 1971

Prepared by

Physics International Company
2700 Merced Street
San Leandro, California 94577

CONTENTS

ILLUSTRATIONS

ILLUSTRATIONS (cont.)

SECTION 1
INTRODUCTION

Utilization of energy available from low-impedance, fast-pulse generators (such as the 1-Ω, 60-nsec FWHM, ≤ 1-MV generator SNARK, Reference 1) requires the development of field-emission diodes with impedance lifetimes ≥ 100 nsec and of beam-transport and energy-density control techniques. Further scaling of generator systems to multi-megampere current levels will require many separate electron beams or one large annular beam to be generated. Again, utilization of the energy from these configurations will necessitate improved techniques for beam transport and concentration at a target location.

The following sections of this paper present the results of experiments in electron beam generation from single and double diodes, and in electron beam transport in both longitudinal and azimuthal external magnetic-field configurations.* Most of the work was performed using two of Physics International's Mylar dielectric pulsed-electron-beam generators: the 1.1-Ω, 350-kV, 350-kA PIML generator and the 1-Ω, 1-MV, 1-MA SNARK generator.

* This work was supported in part by DASA Contracts No. DASA 70-C-0063 and DASA 71-C-0052.

SECTION 2
DIODE STUDIES

Single-diode studies were made of the use of high-current, low-impedance (< 1-Ω) field-emission diodes to allow operation of the generators at or near impedance-matched conditions. When high applied voltages (typically 0.1 to 1.0 MV) are used, the pulsed current in the low-impedance diode is high enough to undergo substantial magnetic self-interaction or self-pinching. This is a feature not included in the relativistic Child-Langmuir treatment of space-charge-limited flow in a planar diode. Our diode physics experiments therefore have aimed at clarifying the relationship between diode voltage, current, and geometry in the low-impedance, high v/γ regime.

Planar, cylindrically symmetric, annular cathodes opposite a stretched foil anode in the SNARK or PIML Mylar stripline machines were used to measure the dependence of diode impedance on cathode radii r_{in} and r_{out}, anode-cathode distance d, and applied voltage $V_o(t)$. Annular cathodes ($r_{in} > 0$) were used for two reasons: to explore diode behavior at fixed outer radius but variable total area; and to extend impedance lifetimes by preventing the early-time anode-cathode shorting that results when the pinched beam vaporizes, ionizes, and generally explodes the anode foil near the axis (Reference 2). Cathodes with roll-pins (Figure 1a) or sharp circular ridges (Figure 1b) as emission surfaces were used to determine whether surface structure can affect impedance. The total diode current $I_o(t)$ was time-resolved

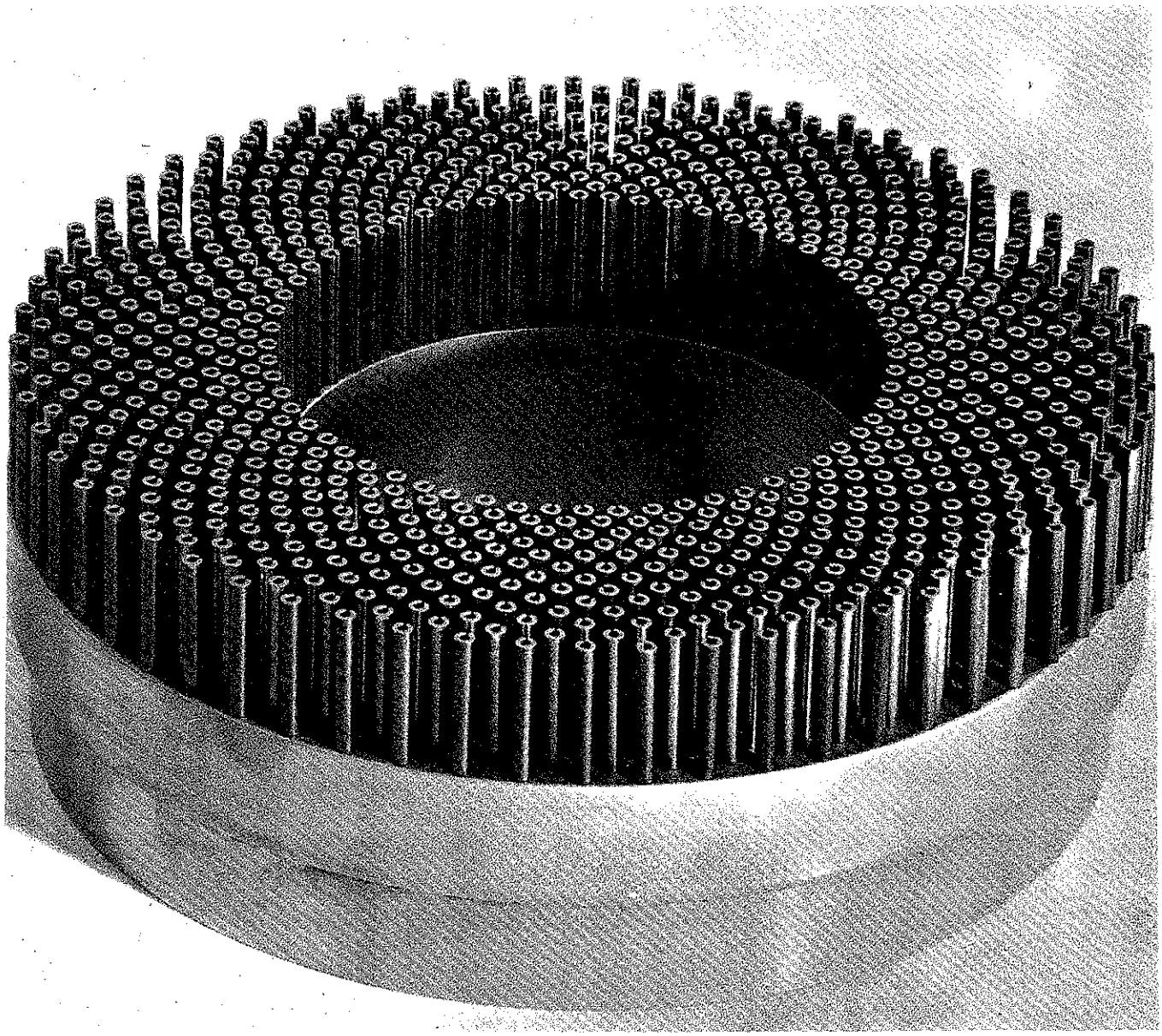

Figure 1a Roll-pin cathode, 14.5 cm diameter. Cathode dimensions were changed on different shots to measure diode geometry dependence.

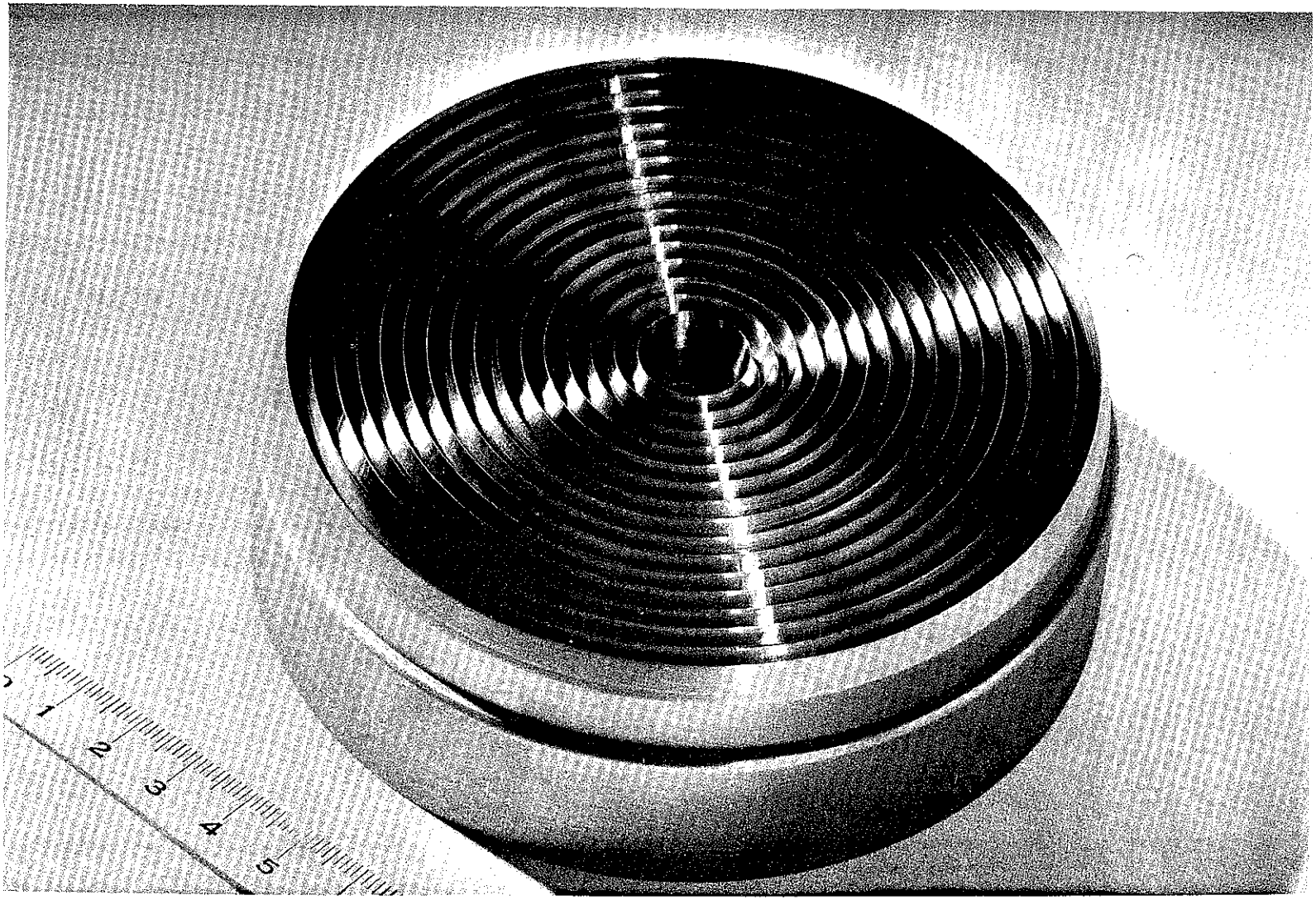

Figure 1b Circular ridge cathode, 11.2 cm diameter. Cathode dimensions were changed on different shots to measure diode geometry dependence.

using a calibrated self-integrating Rogowski coil in the cylindrical wall around the cathode, and the voltage $V_o(t)$ was time-resolved using capacitive dividers in the strip transmission lines that constitute the pulse-forming network. Their outputs were corrected for inductive voltage contributions (flux linkages in the monitor circuit). The diode impedance was $Z(t) \equiv V_o(t)/I_o(t)$. Figure 2 shows the data from two representative pulses. Diode impedance lifetime was typically 110 nsec; at $t \cong 110$ nsec the anode-cathode gap would short, as mentioned above, manifesting a sudden current surge and voltage drop. Past experience has shown that the impedance lifetime can be extended arbitrarily by increasing the anode-cathode distance and by simultaneously increasing the cathode size to avoid the increase in impedance that would otherwise result from this. In what follows we are concerned with diode behavior prior to this collapse of impedance.

The data obtained to date give strong support for the para-potential model of the high-aspect-ratio, high-current diode developed by de Packh (Reference 3), Friedlander et al. (Reference 4), and Creedon (Reference 5). This model depends on the existence of a class of electron trajectories in the diode that are force free. The possibility of such a class existing is supported by the following argument: In beam pinch, electrons emitted near the cathode outer edge, $r = r_{out}$, move to a much smaller radius as they traverse the anode-cathode gap. Such an accumulation of charge near the axis must depress the axial electric field at the cathode at interior radii, so that electron emission is predominantly from the cathode periphery. The instantaneous equipotentials of the applied field are as shown in Figure 3a. The electric force is of course perpendicular to the equipotentials. An electron moving radially inward along a single equipotential also experiences a magnetic force (due to

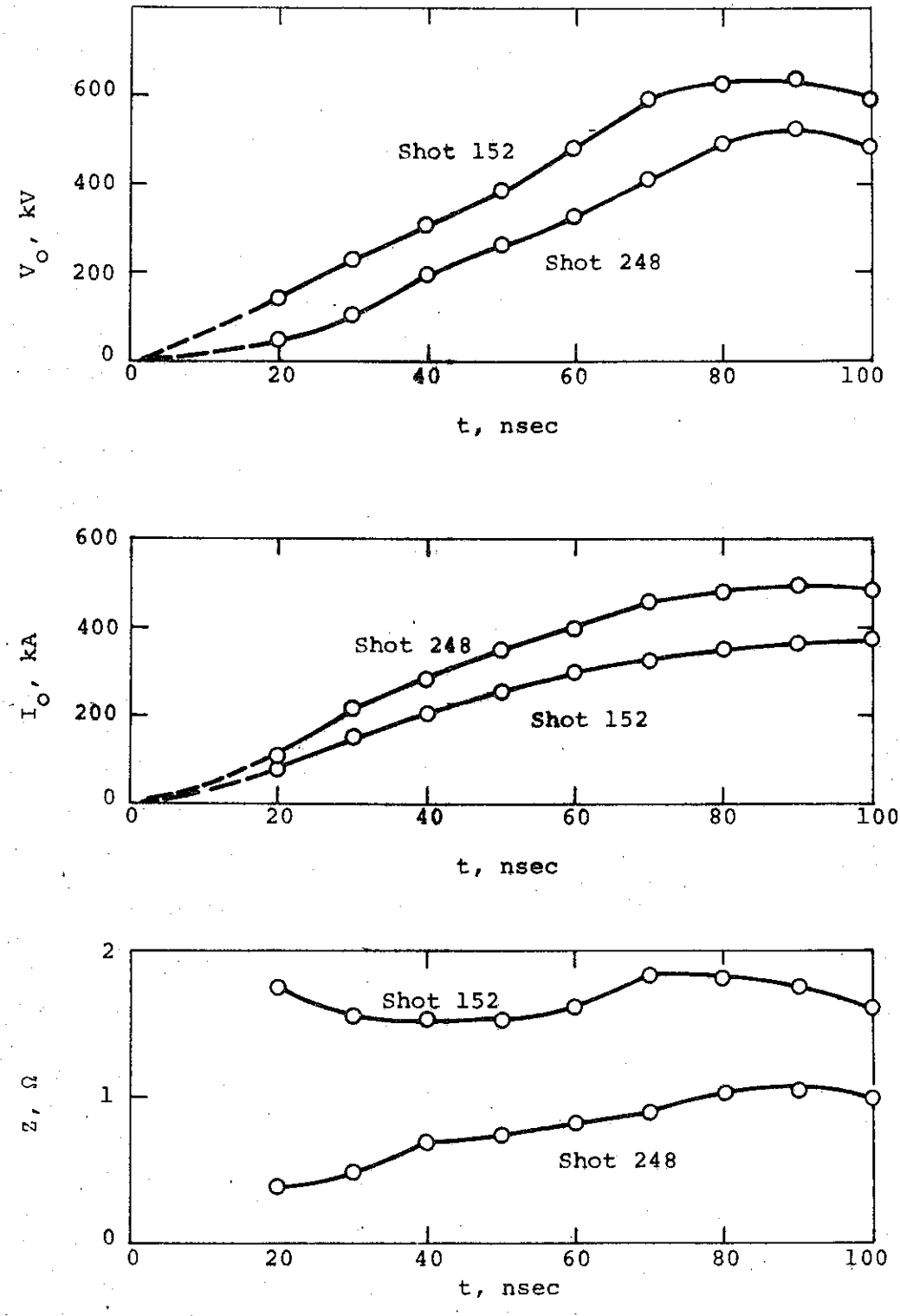

Figure 2 Typical numerical data from two pulses. Voltages and current waveforms were the measured quantities; the impedance $Z(t) = V_o(t)/I_o(t)$. Expansions of anode and cathode plasmas caused impedance collapse (current surge, voltage drop) at typically t = 110 nsec.

the azimuthal magnetic field B_θ) that is also perpendicular to the equipotential and is opposite the electric force. These two forces will be of equal magnitude and cancel each other if the electron velocity divided by the speed of light is $\beta = E/B_\theta$; in such a case, no net force acts on the electron, and its motion is force free as well as parapotential. (This is similar to the situation in a magnetron where the magnetic field acts as an insulator in the interelectrode space.) The assumption of steady-state ($\partial I_o/\partial t = 0$), parapotential, force-free flow provides partial information on the spatial dependence of the current density, charge density, and fields. The added requirements of Ampere's law and Poisson's equation result in the fundamental equation of the flow (de Packh, Reference 3):

$$\nabla^2 V = 2r^{-2}\, dI^2/d^2V \qquad (1)$$

where r is the radius in cylindrical geometry, $V = V(r,z)$ is the potential, and $I = I(r,z)$ is the total current flowing within radius r through the plane z = constant. In simplified cases ($\partial/\partial r >> \partial/\partial z$ or $\partial/\partial z >> \partial/\partial r$, the latter being relevant to the high-aspect-ratio diode of concern here) solutions to Equation 1 indicate that a bias current must travel in the axial direction inside the parapotential flow in order that the conditions for the flow be satisfied. The bias current, arbitrary except for a lower limit, is included in the current I in Equation 1; analytically it is a parameter whose physical origin is outside the theory as it now stands. De Packh has shown that the minimum allowable bias current corresponds to electron parapotential flow along all equipotentials, including those grazing along the anode. Higher bias currents constrain the flow to lower-lying equipotentials (away from the anode), raising the impedance of the diode.

A simple picture due to Creedon (Reference 5) that facilitates application of this analysis to high-aspect-ratio planar diodes is shown in Figure 3b. The equipotentials of Figure 3a are idealized into conical surfaces over most of the interelectrode region. Flow near the cathode edge, where electrons jump to the various equipotentials, and near the axis, where Figure 3b is unphysical, involves orthopotential flow but is not considered to affect the parapotential flow in most of the diode volume. Creedon treats the grazing case mentioned above and finds the voltage-current characteristics shown by the smooth curve in Figure 4, for which

$$I_o = 8500\ (r_{out}/d)\ \gamma_o\ \ln\left[\gamma_o + (\gamma_o^2-1)^{\frac{1}{2}}\right]\ \text{(mks)}\quad (2)$$

where

$$\gamma_o = 1 + eV_o/mc^2$$

Diode measurements for $\partial I_o/\partial t = 0$ ($I_o = I_o^{max}$) are also shown in Figure 4. They agree with the steady-state parapotential calculations over the ranges of $7.26 \leqslant r_{out}/d \leqslant 20.8$, $370\ \text{kV} \leqslant V_o \leqslant 970\ \text{kV}$. The type of cathode surface used--roll-pin or concentric circular ridge--does not appear to be discernable from the data. This gives added support to the view that beam electrons originate at the cathode periphery rather than from the planar cathode surface.

If, as seems reasonable at this point, this means that grazing parapotential flow occurs in these diodes, how do electrons come to populate the equipotentials "correctly"? Is there a real bias current; what is its physical nature; and why does it have the value that corresponds to the grazing case? One possibility for the bias current is that positive ions from the anode are accelerated toward the cathode along the axis. The

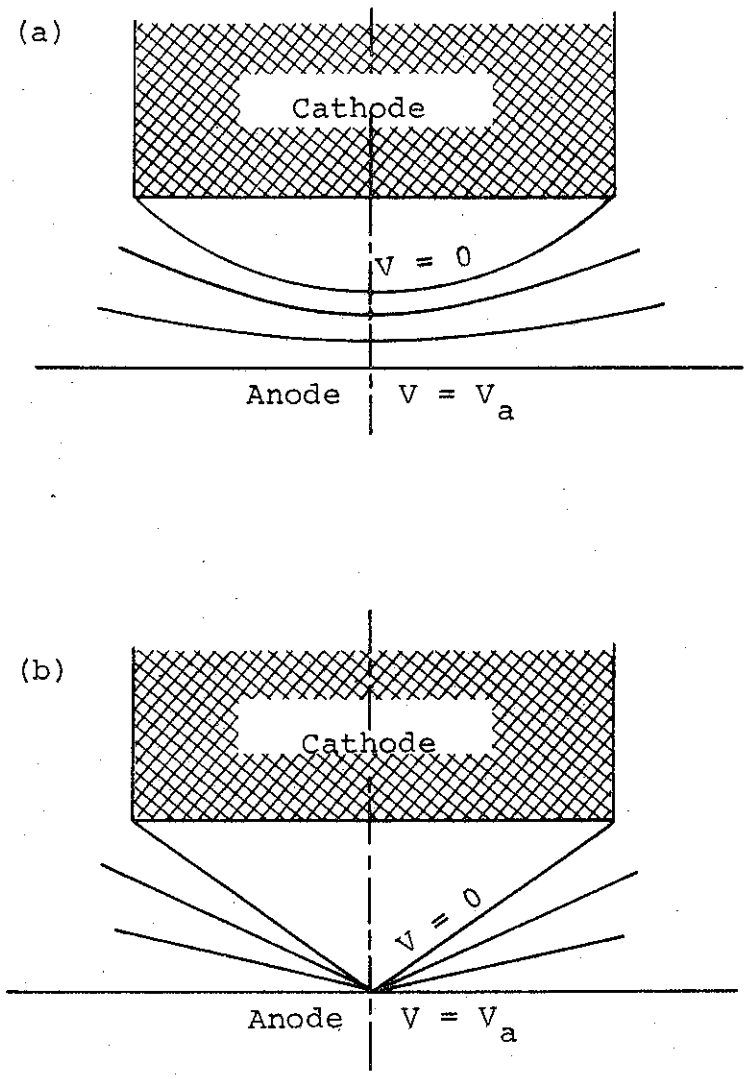

Figure 3 Equipotentials due to hypothetical steady-state voltage applied across diode: (a) physical schematic - electric field is suppressed over most of cathode surface due to beam pinch, (b) idealized geometry for parapotential flow calculations.

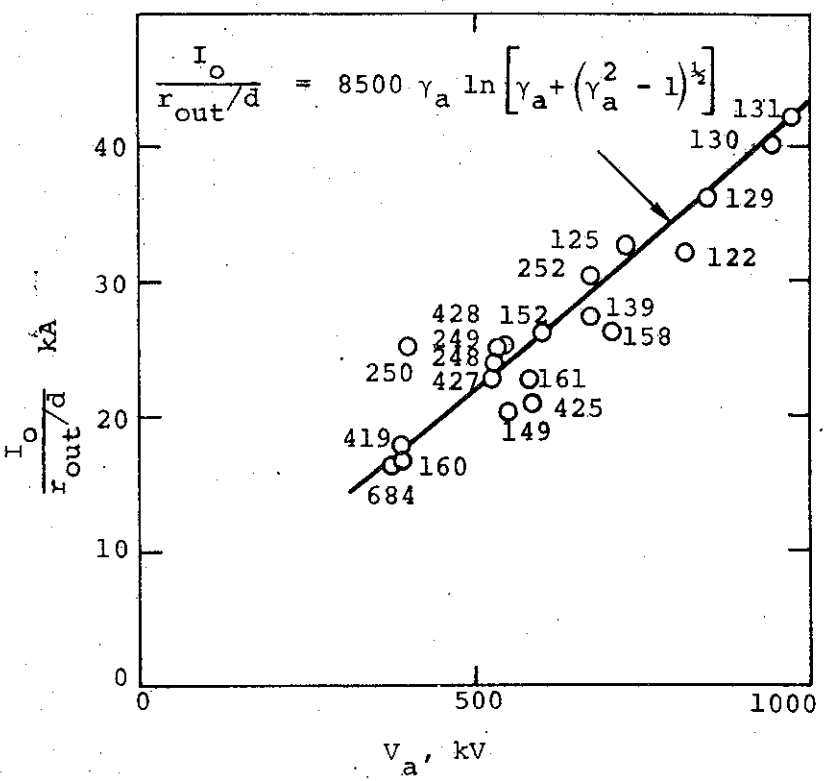

Pulse no.	$\frac{r_{out}}{d}$	Cathode type*	Cathode r_{out}	Cathode r_{in}	anode	gen.
122	19.8	R.P.	5.9	3.3	2-mil Ta	Snark
125	16.9	R.P.	5.9	3.3	2-mil Ta	Snark
129	16.9	R.P.	5.9	3.3	2-mil Ta	Snark
130	18.3	R.P.	5.9	3.3	2-mil Ta	Snark
131	19.8	R.P	5.9	3.3	3-mil Ta	Snark
139	18.3	R.P	5.9		2-mil Ta	Snark
149	15.9	C.R	5.6	2.7	2-mil Ta	Snark
152	14.0	C.R.	4.9	3.7	2-mil Ta	Snark
158	12.3	C.R.	5.6	4.6	2-mil Ta	Snark
160	12.3	C.R.	5.6	4.6	2-mil Ta	Snark
161	15.9	C.R.	5.6	3.7	2-mil Ta	Snark
248	20.4	C.R.	7.2	4.6	2-mil Ta	Snark
249	20.8	R.P	7.3	3.9	2-mil Ta	Snark
250	20.4	C.R.	7.2	4.6	2-mil Ta	Snark
252	20.8	R.P	7.3	3.9	2-mil Ta	Snark
419	22.4	R.P	7.3	3.9	2-mil Ta	Snark
425	22.4	R.P	7.3	3.9	2-mil Ta	Snark
427	22.4	R.P	7.3	3.9	¼-mil Al-My	Snark
428	20.8	R.P	7.3	3.9	¼-mil Al-My	Snark
684	7.3	R.P	1.8	0	1-mil Al	PIML

*R.P. = Roll-pin, C.R. = Concentric ridge

Figure 4 Comparison of the current-voltage characteristic as predicted by the steady-state parapotential analysis with measured values. For this comparison the data are restricted to $\partial I_o/\partial t = 0$: $I_o = \left[I_o(t)\right]_{max} = I_o(t_m)$, $V_o = V_o(t_m)$; each experimental point (I_o, V_o) comes from a single beam pulse.

region of flow near the axis has not been physically modeled. Does the beam really funnel along the equipotentials down to a small spot when $\partial I_o/\partial t = 0$ or does the beam current density versus radius at the anode plane have wings that extend out to the cathode radius? The analytical and experimental clarification of these questions is important at this point in the understanding of very high-current diodes.

The data shown in Figure 4 pertain to steady-state conditions where $I_o = I_o^{max}$. As described earlier, the current and voltage measurements were time-resolved, as in Figure 2. During the risetime of the current, when $\partial I_o/\partial t \approx 5 \times 10^{12}$ A/sec, I_o is greater than the value predicted by Equation 2. A representative example is shown in Figure 5. To explain why this occurs, a time-dependent parapotential flow analysis is needed.

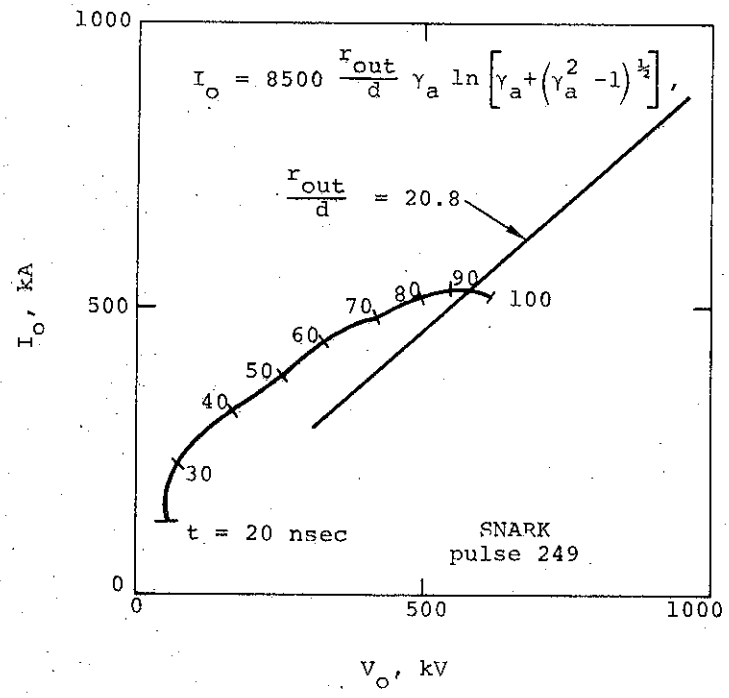

Figure 5 Measured $(V_o(t), I_o(t))$ trajectory for pulse 249.

Double-diode studies consisted of testing the physical basis of magnetic isolation. Cathode shanks were 3 inches in diameter and were 2.86 centimeters apart. As shown in Figure 6, each cathode was directly exposed to the magnetic field of the other over a 2-centimeter length at the cathode base. In addition, it can be seen that each cathode in its cylindrical conducting enclosure can be viewed as a coaxial transmission line in that the beam current flowing along the shank will induce a reverse current in the surrounding wall. For a single-cathode configuration, the induced return current is azimuthally uniform as it leaves the cathode enclosure and flows radially away along the inside surface of the horizontal anode support plate. For a double-cathode arrangement, however, the induced return current in each cylinder wall must be strongly peaked opposite the central

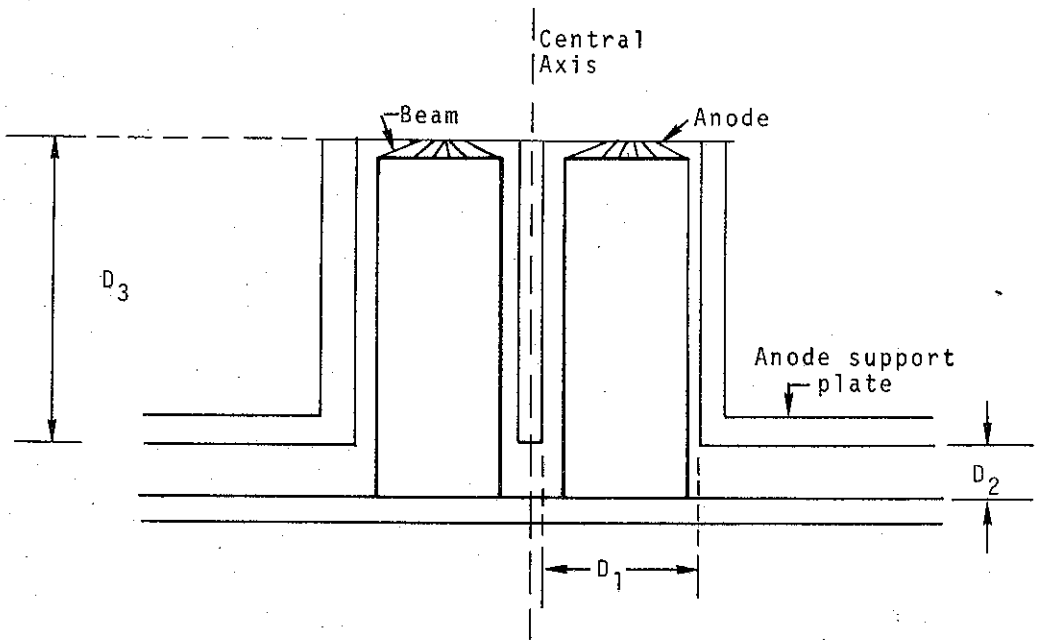

Figure 6 Magnetic isolation of adjacent diodes.

axis, near which it must be zero. This effect causes the current to flow primarily along the inside portion (near the central axis) of each cathode, as does the direct exposure of each cathode to the magnetic field of the other in the gap D_2. In order to generate unperturbed, uncoupled beams, the ratio D_3/D_1 (or D_3/D_2, if D_2 is larger than D_1) must be sufficiently greater than unity, so that the cathode current-flow asymmetries, strongest near the support plate, are negligibly transmitted to the anode-cathode gap where the beam is generated. By changing D_3 the ratio D_3/D_1 was adjusted to be 0.312, 0.625, and 3.12. In the first two cases, graphite witness plates showed damage craters that were close together than the cathode axes, with the strongest mutual attraction when $D_3/D_1 = 0.312$. However, $D_3/D_1 = 3.12$ gave damage craters on line with the respective cathode axes, indicating complete isolation of the beams.

SECTION 3
BEAM TRANSPORT STUDIES

High-current electron beams are injected into a transport region by choosing a small anode thickness compared to the electron range. Beam propagation in the transport region depends on the properties of the fill gas and the externally applied field configuration, if any. Studies of intense beam propagation in neutral gas have shown this process to be lossy (Reference 6). The back emf generated by the fast-rising magnetic field of the beam decelerates beam electrons. One solution to this problem is to preionize the gas in the transport region. In this way the back emf is shorted out by the conductivity of the medium which produces an induced back current of secondary electrons. However, this back current effectively neutralizes the self-magnetic field and the unconstrained beam expands quickly to the walls (Reference 7). To trap magnetic fields in the background plasma to constrain the beam, either azimuthal (B_θ) or longitudinal (B_Z) fields can be used.

3.1 B_θ SYSTEMS

A conducting plasma with a trapped B_θ field can be produced by a linear pinch. With this configuration the anode of the beam-generating diode and the cathode of the Z-pinch are the same thin foil so that the beam enters the pinch directly (Figure 7). Thus the beam and pinch current are parallel and the pinch magnetic field acts to constrain the beam. The bear is transported down the collapsing plasma column striking the pinch anode plate and producing X-rays by which transport efficiency is measured.

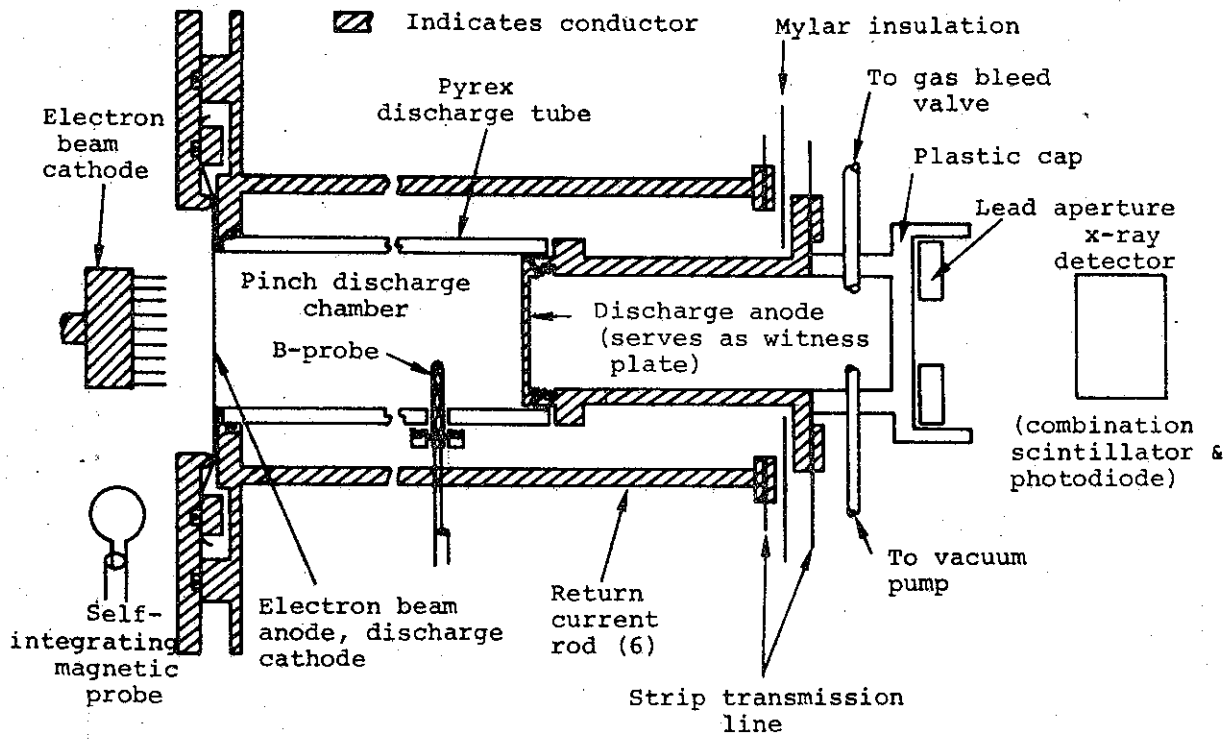

Figure 7 Experimental configuration of Z-pinch apparatus and beam-generating diode

Using this technique, a series of experiments have been performed with the pinch radii varying from two to four inches, and the length from one to two feet (Reference 8). Beams with peak currents of 120 kA, 140 kA, and 160 kA, with corresponding mean energies of 750 keV, 625 keV and 500 keV, were injected into a collapsing pinch discharge. Transport of these beams was complete as evidenced by the preservation of both the amplitude and shape of the X-ray signal produced in the pinch anode (Figure 8). Virtually complete neutralization of the self-magnetic field of the beam was inferred from the low induced voltage across the pinch electrodes; (the appearance of any net current due to the beam must produce an L dI/dt voltage drop). The size of the damage patterns at the pinch anode showed that the beam propagated inside the collapsing pinch-current sheet (Figure 9). This allowed the fluence of the beam at the target to be varied by varying the time of beam injection into the pinch.

Recent experiments have extended this technique to 300-kA, 600-kV SNARK beams. An 8-inch pinch, 1-1/2 feet long and having a maximum current of 750 kA, was used to obtain beam transport and fluence control. Figure 10 shows magnetic field profiles for four times of beam injection. Figure 11 shows that again diode damage occurred on the inside of the current sheet during collapse. Transport efficiency was greater than 90 percent. Varying the injection time from 0.95 μsec to 5.6 μsec changed the area of the damage pattern from 250 cm^2 to 50 cm^2, showing the extensive fluence control available with this technique.

The results of the above experiments may be understood as follows: Current neutralization quenches the self-field of the injected beam. The electrons of the beam are therefore decoupled

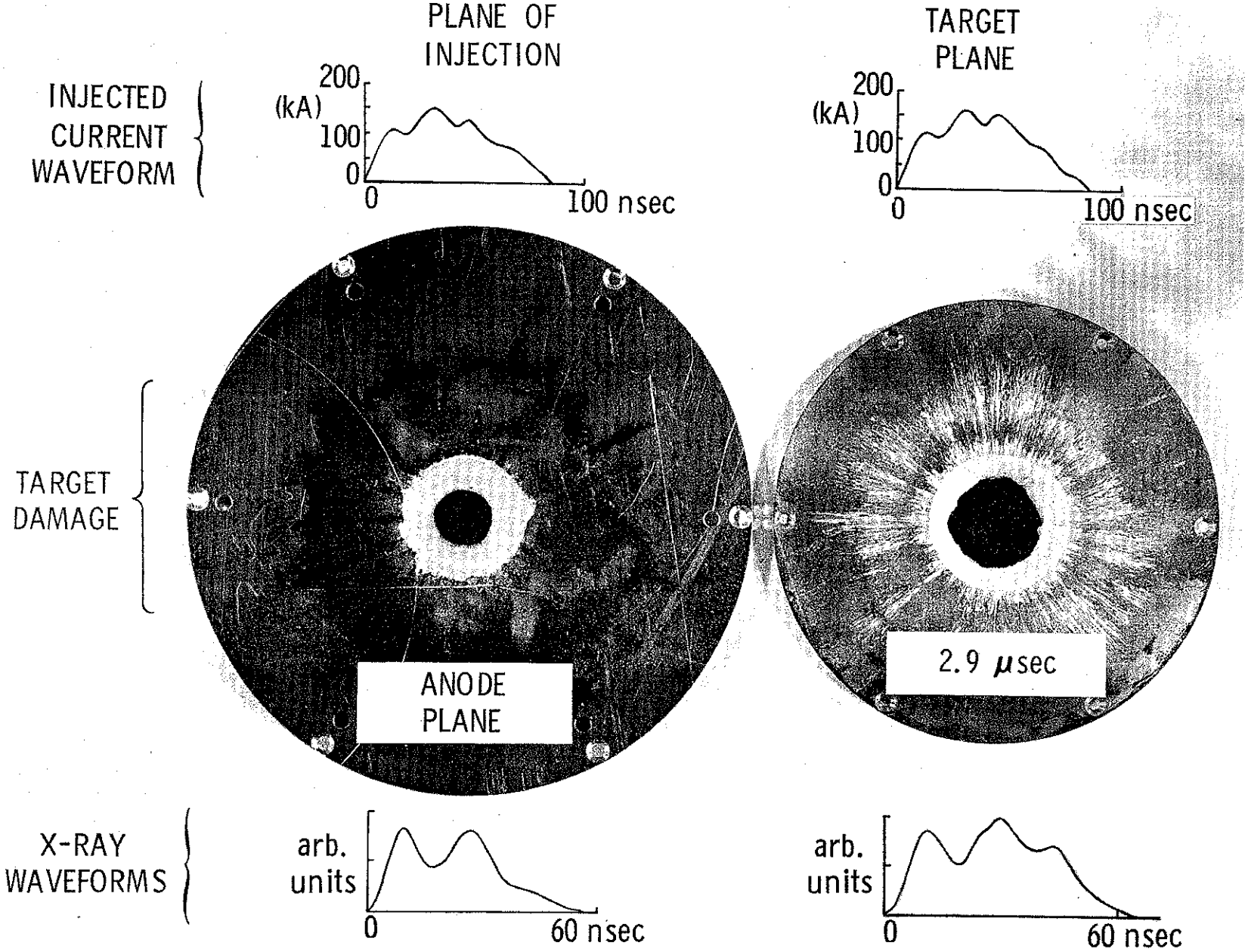

Figure 8 Transport of 160 kA beam. Last half of transported beam has slightly higher current and voltage than reference beam, resulting in more intense bremsstrahlung. Hole and overall damage diameters indicate that beam expanded during propagation.

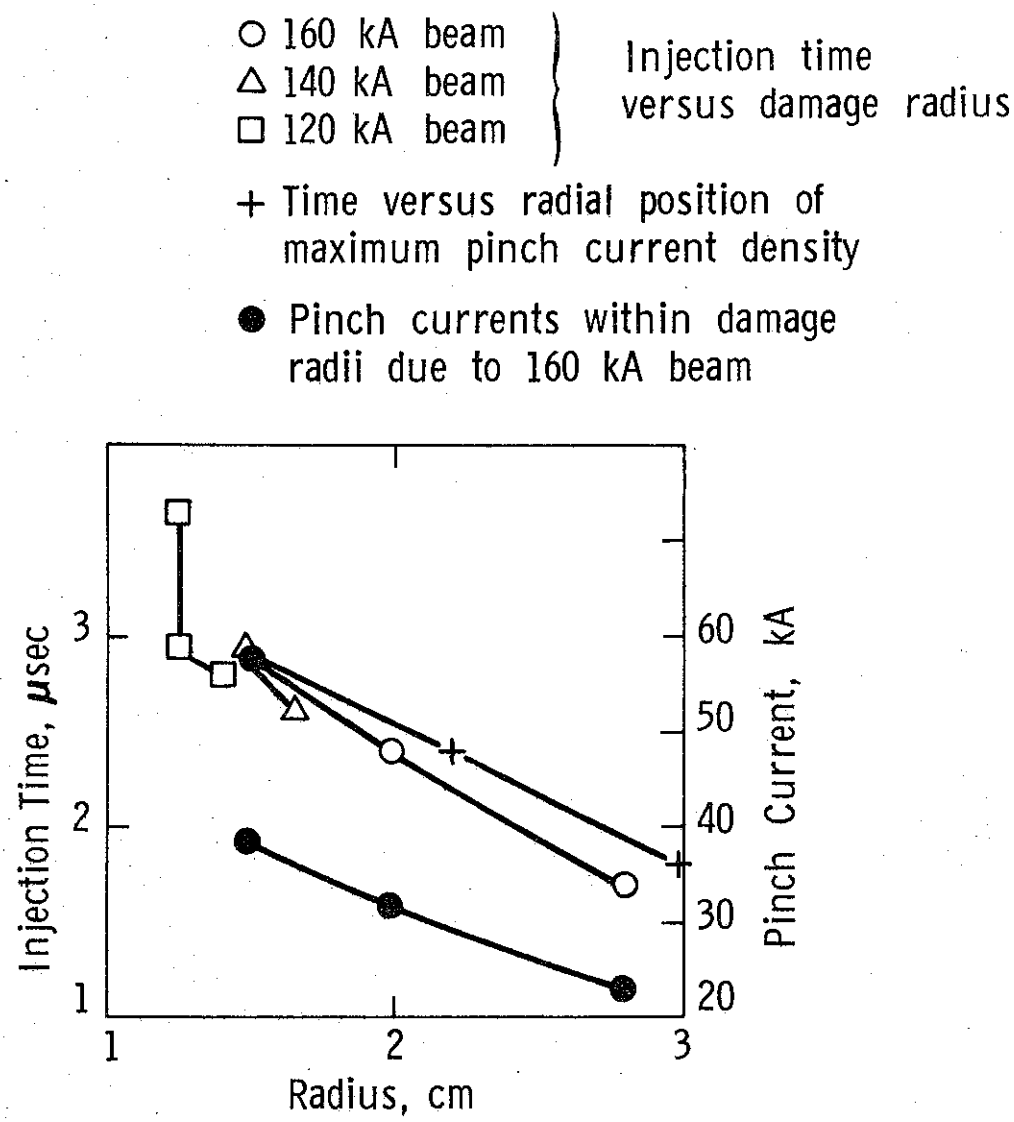

Figure 9 Graph showing damage radii, injection times, collapse trajectory of pinch current sheet, and amounts of pinch current inside damage radii of 160 kA beams.

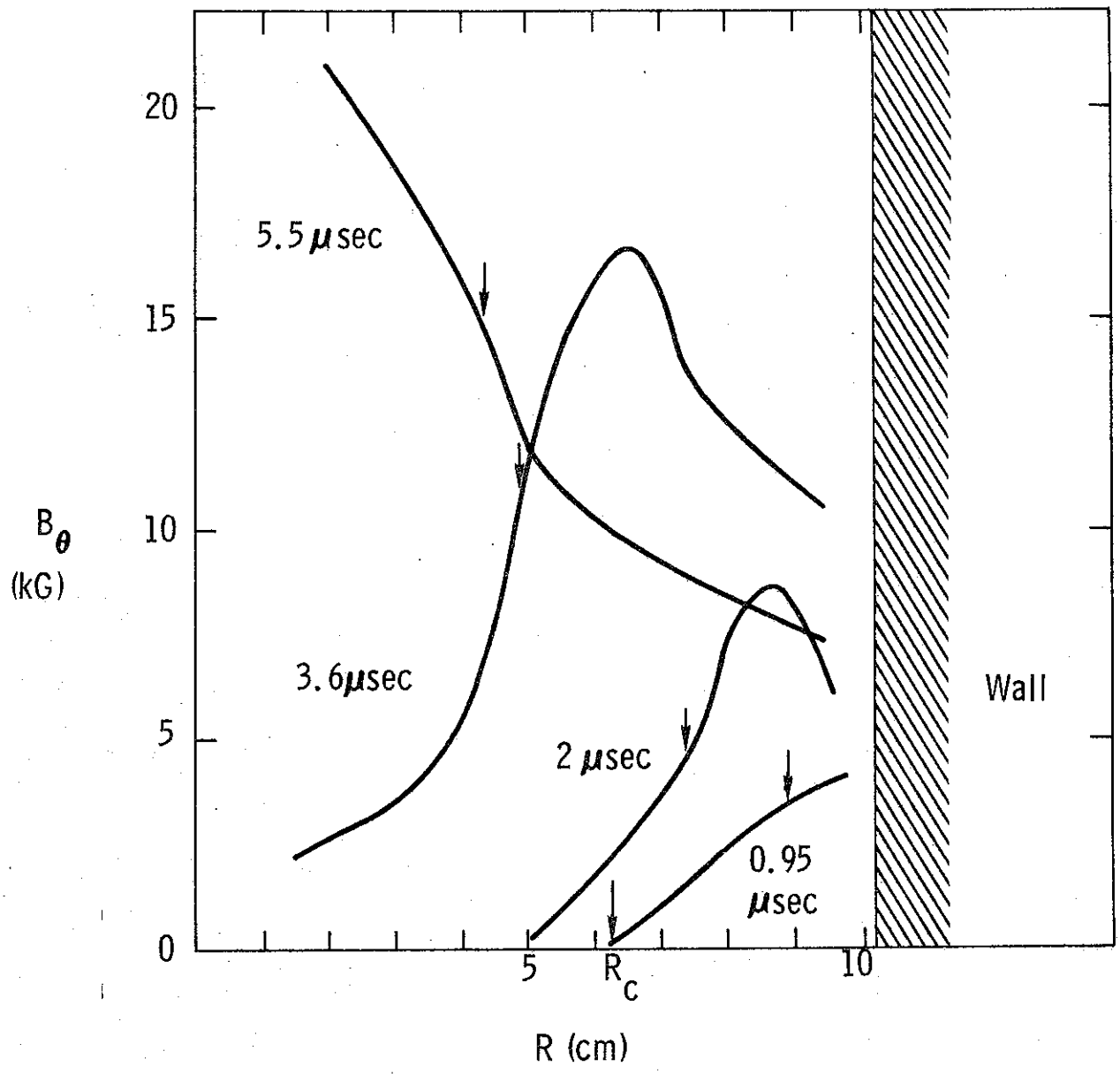

Figure 10 Magnetic field profiles at times of beam injection. R_c is beam cathode radius, arrows indicate damage radii of transported beams.

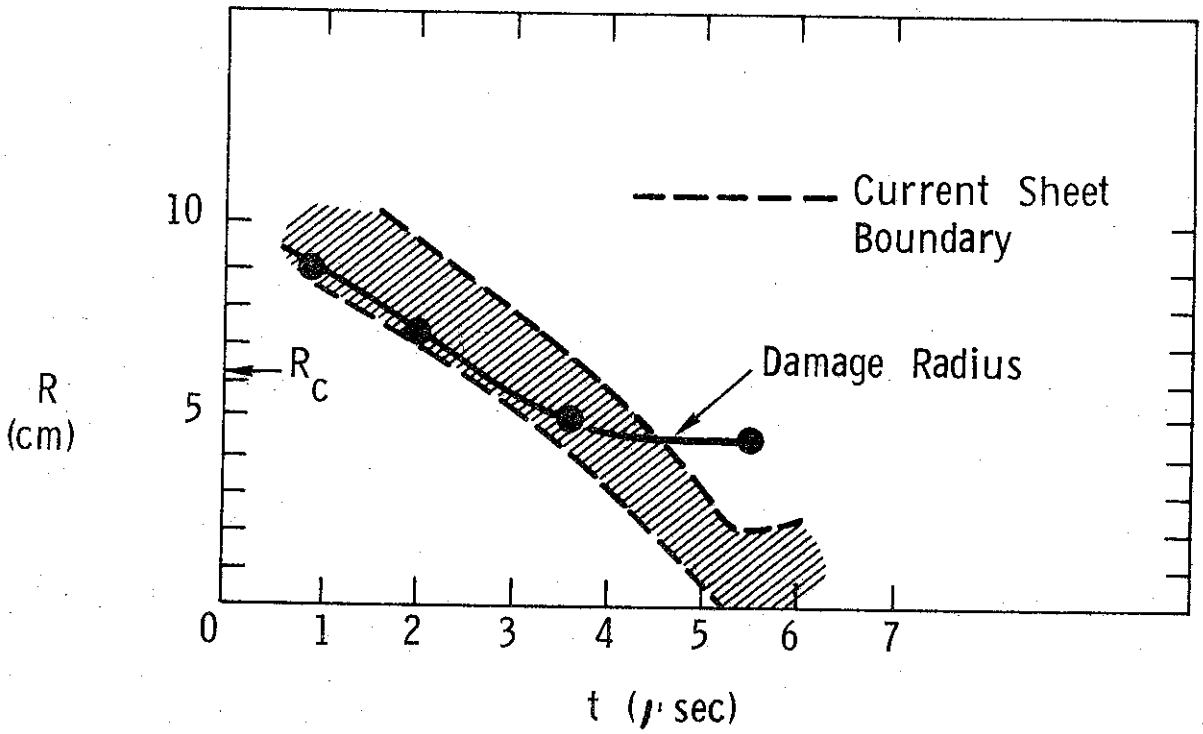

Figure 11 Pinch anode damage radii as a function of beam injection time.

from each other. To the extent that the pinch current sheet is sharp, beam electrons follow single-particle orbits and are deflected at the inner edge of the current sheet by its magnetic field. They fill the inside of the current sheet as if they were inside a perfectly reflecting tube. In Figure 12, a typical field profile for a linear pinch is shown. In region I beam electrons execute periodic orbits about the axis of the pinch as just described. Region I is that radius interval wherein the pinch current is insufficient to turn a beam electron back into the diode. For a linearly rising field profile, this critical current would be the Alfven current $I_A = 17{,}000\ \beta_{\|}\gamma$. For field profiles more like that of the pinch (such as considered by Hammer and Rostoker, Reference 9), the enclosed current could be greater. (Note that in both Figures 9 and 10, pinch current enclosed by the beam channel is always of the order of the Alfven critical current.)

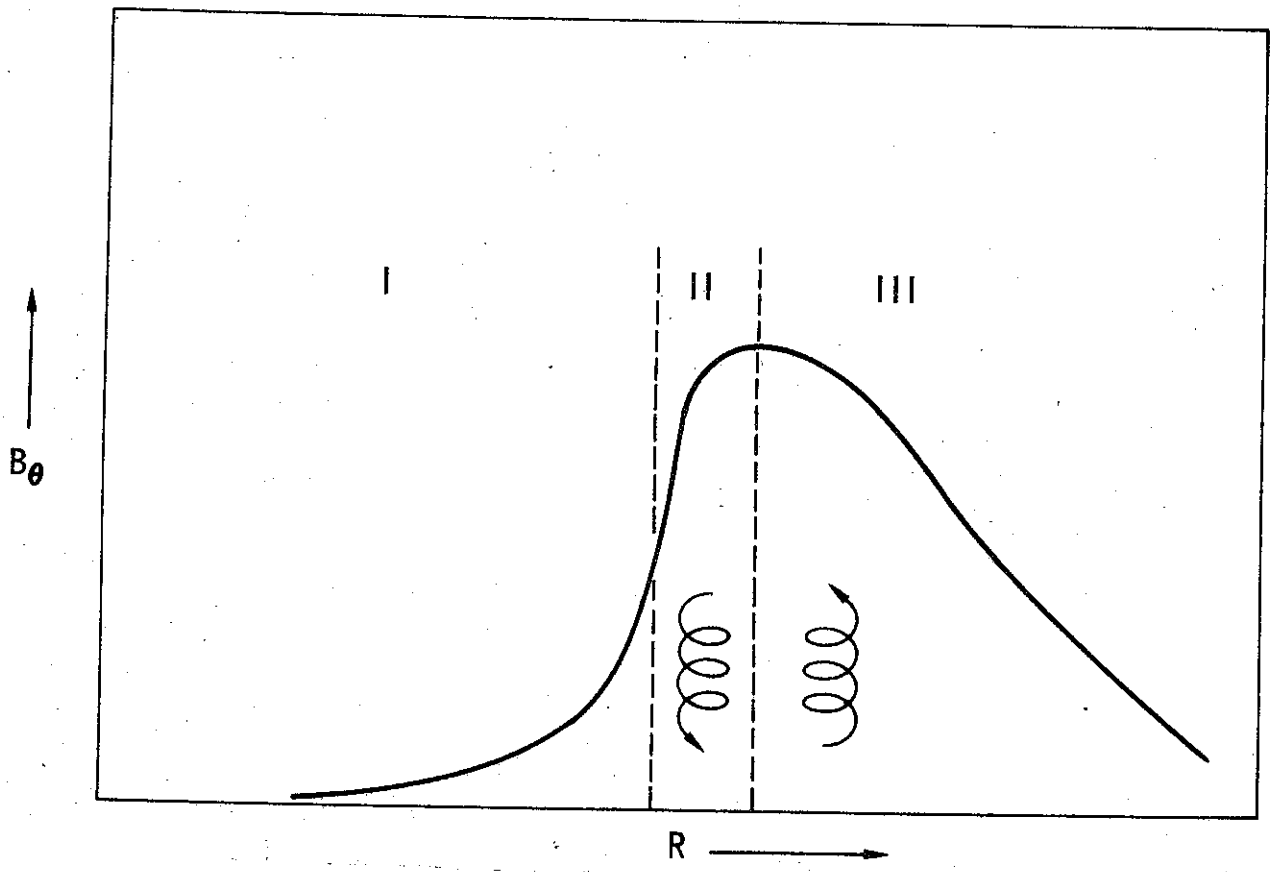

Figure 12 Typical field profile for collapsing linear pinch current sheet.

However, this is not the only mode of transport possible. In region II of Figure 12, where the enclosed pinch current is greater than I_A and $\partial B_\theta/\partial r > 0$, beam electrons undergo a ∇B drift type trajectory which turns them back into the diode. On the other hand, region III, where enclosed current is greater than I_A but $\partial B_\theta/\partial r > 0$, should transport beam current because the ∇B drift is in the right direction. Evidence for this can be seen in Figures 9 (120 kA beam) and 11 where injection at late time, such that much of the beam is injected into $\partial B/\partial r > 0$ regions, allows transport without expansion of the beam. Observation of the existence of region II would be difficult in that

damage to the anode in regions I and III would essentially obliterate any annulus undamaged by the beam itself. Reversal of the pinch current (anti-parallel to beam) would cause transport to be possible only in region II. However, reversal of the pinch current has only been attempted for collapsing pinch profiles where region I received injected electrons. In this case, the beam was expelled quickly to the wall in agreement with expectations.

Since the beam current is neutralized by a background conducting plasma, the only condition for propagation of very high-current beams is that the magnetic field of the pinch be sufficiently strong to turn back the beam particles before they reach the discharge tube wall. For particle energies of about 1 MeV or less, this is easy. However, since the construction of high-current machines demands large cathode areas, the pinch diameter must increase as well. This implies a larger pinch current to produce a given containing field.

The transport mechanism described above offers a simple way to combine beams while transporting them. Two beams to be combined are injected inside a single collapsing current sheet. They are both current neutralized and the electrons of both beams follow their single-particle orbits to the target (Figure 13). The θ-components of velocity resulting from off-axis injection of the high v/γ beams result in their azimuthal mixing, so that the combination beam is soon azimuthally symmetric. The advantage of this scheme is that the beams are mixed, not merely brought into proximity, and cannot be separated later. The need for current sheets large enough to encompass two diodes places a demand on the risetime of the pinch bank and on the size of the pinch tube; but these can be met with present technology.

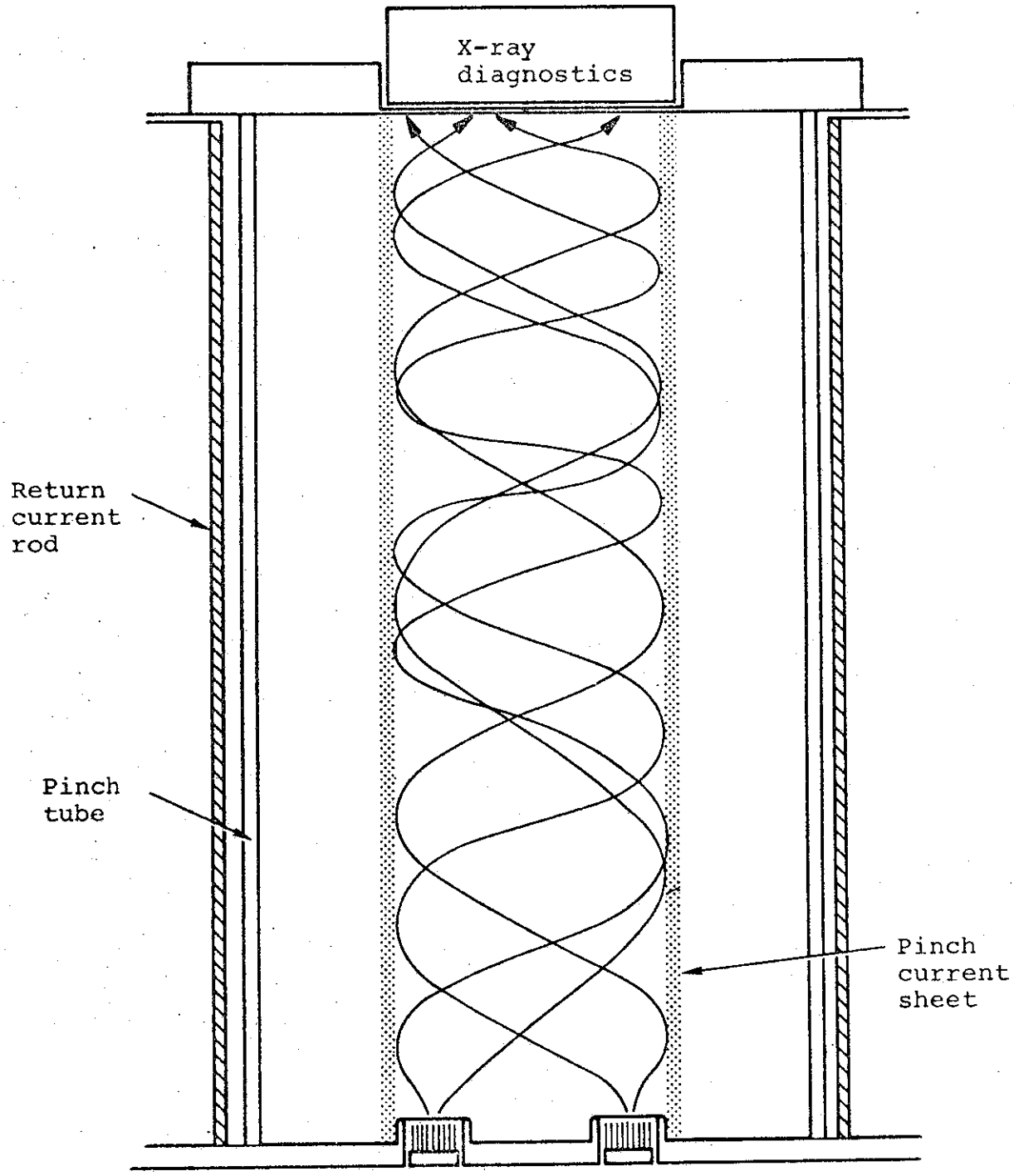

Figure 13 Beam combination in a Z-pinch.

The single-particle model predicts that beam electrons can be funneled or compressed if they are injected into a tapered linear pinch (Figure 14). Beam electrons should be axially reflected if the pinch taper is too severe or the electrons are injected at too large an angle. This is similar to the motion of particles in a magnetic mirror, although no adiabatic invariant is involved. As the tapered pinch collapses, one might expect to see diminishing damage patterns and reduction of propagation efficiency as more particles are reflected, until transport is cut off entirely. An experiment of this type has been completed, however, and the beam was not reflected, although some compression did occur. These data are still under examination, and it remains to be seen if they are compatible with the single-particle model described here.

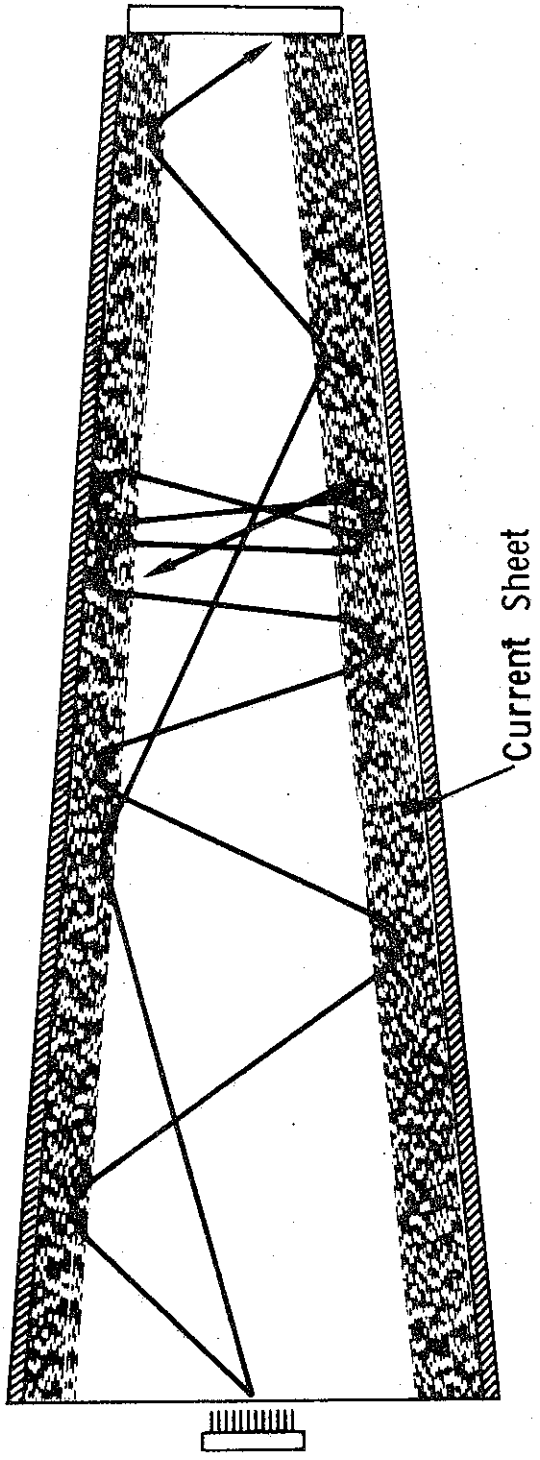

Figure 14 Transmission and reflection of beam electrons in a tapered Z-pinch with a sharp current sheet.

3.2 B_Z Systems

The second method of containing beams in a background plasma is the use of a longitudinal magnetic field. In contrast to the Z-pinch configuration (where an axial current provides both the magnetic field and the plasma), longitudinal field configurations allow the possibility for independent variation of field strength and plasma properties (Reference 10). For these experiments the magnetic field was produced by a long-time constant solenoid, and the plasma was produced by a high-frequency oscillation superimposed on the field coil circuit. In this experiment the high-frequency oscillation was derived from the low-frequency circuit so that the plasma density and field strength were not completely independent, although in principle this is not necessary.

Most of the beam transport experiments with B_Z were carried out over a distance of 0.5 meter using an electron beam with 250-kV mean electron energy and 200-kA peak current (generated by the PIML machine).

This apparatus consists of a solenoid surrounding the beam transport region and a magnetically transparent diode (Figure 15). The solenoid had a uniform field from the cathode to the target with a radial variation of less than three percent over the cathode area. The solenoids were driven by a 48-kJ capacitor bank with a period that was typically 800 microseconds. The

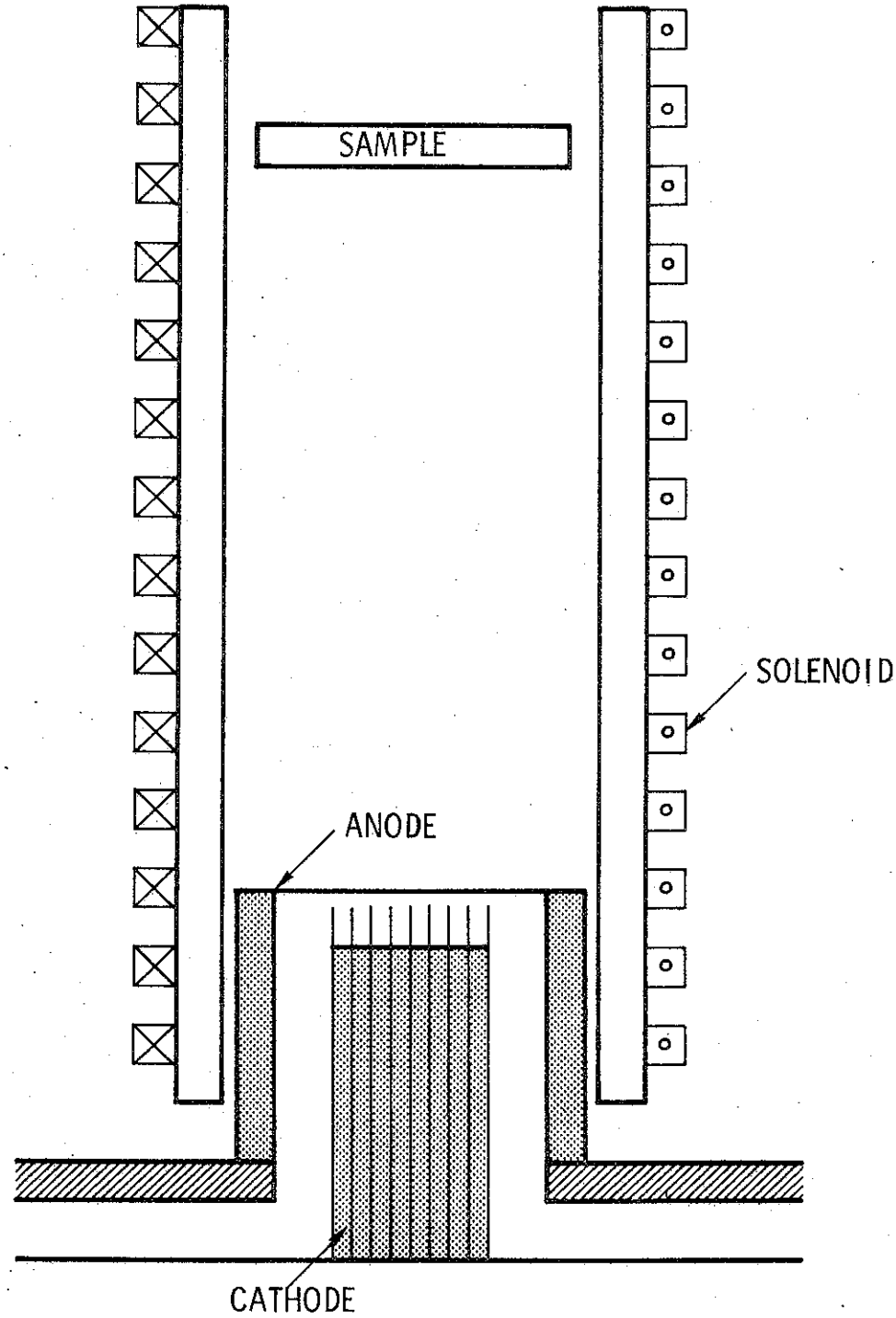

Figure 15 Diagram of the solenoid transport system.

high-frequency oscillation (superimposed on the magnetic field to ionize the dry nitrogen gas fill) was at a frequency of $\approx$ 500 kc. In practice this preionization increased as the magnetic field increased but the plasma density was always in the region of 10^8 to 10^9/cc.

Figure 16 is a summary of the results of these experiments for the PIML beam. When the pressure in the solenoid was 600 millitorr and the magnetic field was not used, the transport efficiency was 42 ± 10 percent. Without the magnetic field, the diode region pinched into a small core and the beam then spread and diffused in the transport region, filling the entire drift tube. When a B_z field was used (fields larger than 4 kG were tested) the beam retained approximately the same shape and size as the cathode. This is shown most dramatically in Figure 17 which pictures the damage pattern produced by a beam generated with a ~ 3-inch-by-1-inch rectangular cathode. The beam transport distance was 25 centimeters. The cathode itself had a somewhat wavy edge since the emission surface consisted of 1/16-inch-diameter rods that were 1/4 inch apart. Although the sample damage area is more irregular than the cathode, the obvious reproduction of cathode shape and area, even after 1 meter of transport, indicated that the transport process can be approximated by a single-particle-orbit theory in which collective effects are ignored in the transport region. This is not to say that collective effects do not take place, but only that they are not the dominant processes in these experiments. Further evidence for a single-particle model was that local non-uniformities in beam fluence at the target were obviously present until the magnetic field was lowered enough for the electron gyro diameter to equal the cathode inter-rod distance. When this condition was satisfied the sample appeared very uniform. When the beam transport distance was increased from 0.5 meter to 1 meter, the transport efficiency changed by less than 10 percent.

TRANSPORT EFFICIENCY FOR 0.5 METER
(errors are ± 10%)

t = 150 μsec

Pressure (millitorr)

B_z (k gauss)	200	600	1000
4.1	65%	92%	93%
8.25	92%	98%	60% 100%
13.7	69%	72%	75%

t = 240 Msec

Pressure (millitorr)

B_z (k gauss)	200	600	1000
8.4	100%	98%	93%
14.0		100%	

t refers to the time after the start of the applied B_z field.

Figure 16 Beam transport at 0.5 meters for the PIML electron beam. The peak current was 200 kA and the mean energy was 250 kV.

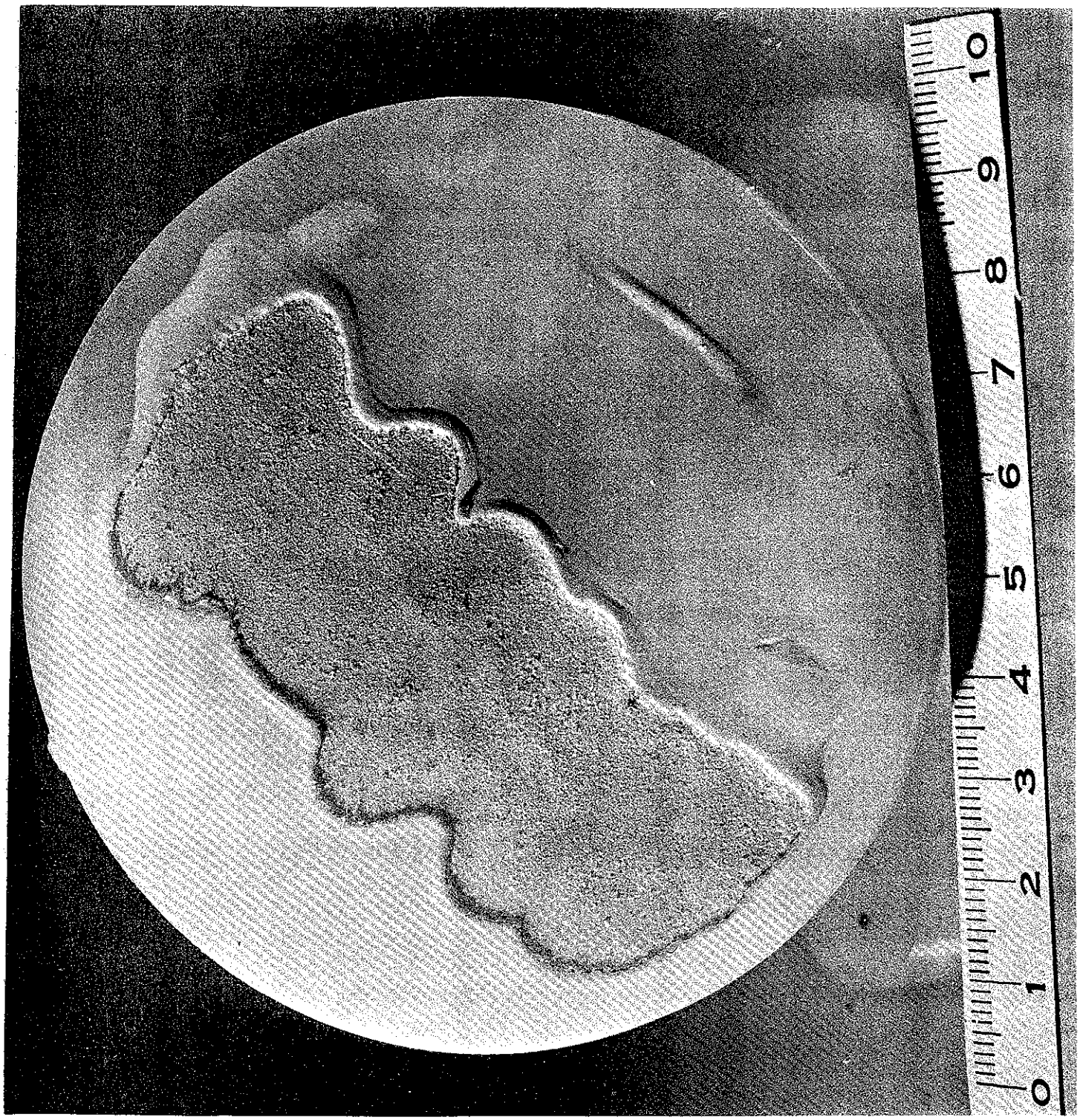

Figure 17 Damage crater in polyethylene produced by a beam generated with a 3-inch by 1-inch rectangular cathode. The beam transport distance was 25 centimeters.

A262

Experiments were also carried out to study the effect of applied longitudinal magnetic fields in the diode. Figure 18 is a comparison of X-ray pinhole photographs of a three-inch-diameter rod cathode with three different field strengths. Two observations can be made: First, the cathode structure is discernable in even the lowest external field, and second, the current density appears higher near the cathode center at all field levels studied. Because of the first observation, the second one cannot be explained by the assumption of beam self-pinch, since the latter characteristically does not preserve cathode surface structure. To explain the observed effects, we propose an explanation of diode behavior when B_z is of the same order as $(B_\theta)^{max}$. The magnetic field in the diode is the sum of the applied uniform axial field and the azimuthal self-field, which increases with radius. The net field, therefore, is helical, and the pitch decreases as radius increases. Assuming that the electrons in some sense follow the field lines, the electron axial velocity is a decreasing function of radius, and the time spent in the diode by an electron is an increasing function of radius. The space-charge-limited current density would therefore decrease with increasing radius for a given anode-cathode voltage. To test this hypothesis, a hollow-core multirod cathode with a 3-inch outer diameter and a 1-inch hollow core diameter was tested. If the beam were pinching due to its own self-field, the highest current density would be at the central axis; but if the above arguments apply, then the current density would be highest directly over the innermost emitters and would be zero over the 1-inch-diameter hollow core. This type of behavior is evident in Figure 19, an X-ray pinhole photograph taken using this hollow cathode. The self-field of the beam at the edge of the cathode was 10 kG and the longitudinal magnetic field was 11.8 kG. This supports the model presented above.

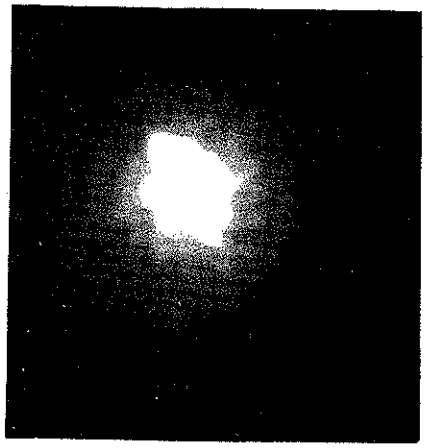

B_z = 3.8 kg

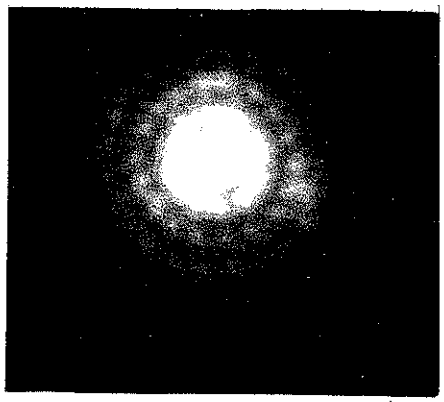

B_z = 6.0 kg

B_z = 7.9 kg

Figure 18 X-ray pinhole photographs of the anode using a 3-inch diameter rod cathode: (a) B_z = 3.8 kG, (b) B_z = 6.0 kG, and (c) B_z = 7.9 kG.

Since the current density is highest at the innermost cathode emitters, the diode impedance should not be sensitively dependent upon cathode area (when the latter is above a certain critical value). Figure 20 shows impedance as a function of time for a 3-inch-diameter cathode and a 3-inch-by-1-inch rectangular cathode. Even though their areas are different by a factor of 2.3, their impedances are approximately equal. In the limit $B_z >> B_\theta$, the field is approximately axial over the entire cathode and emission is approximately uniform, so that the impedance is sensitive to the cathode area.

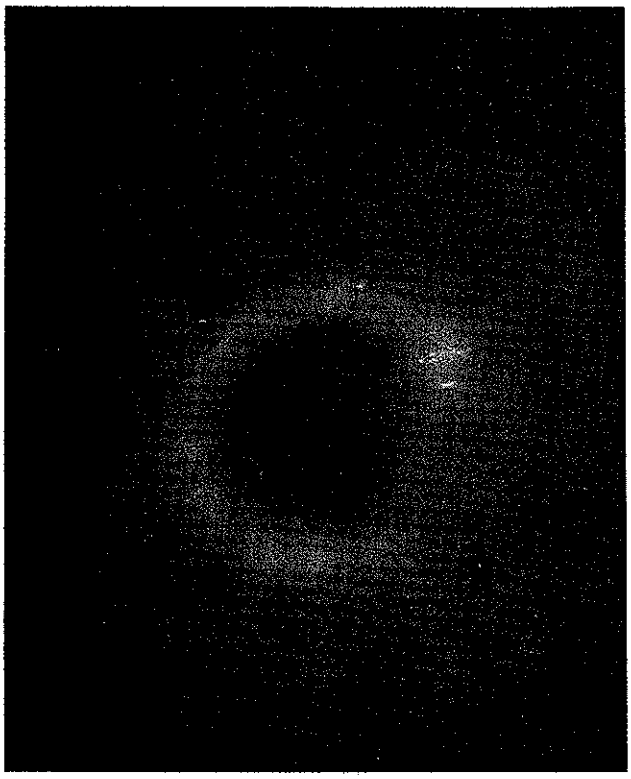

Figure 19 X-ray pinhole photograph of the anode using a hollow cathode three inches in diameter with a 1-inch-diameter hole in the center.

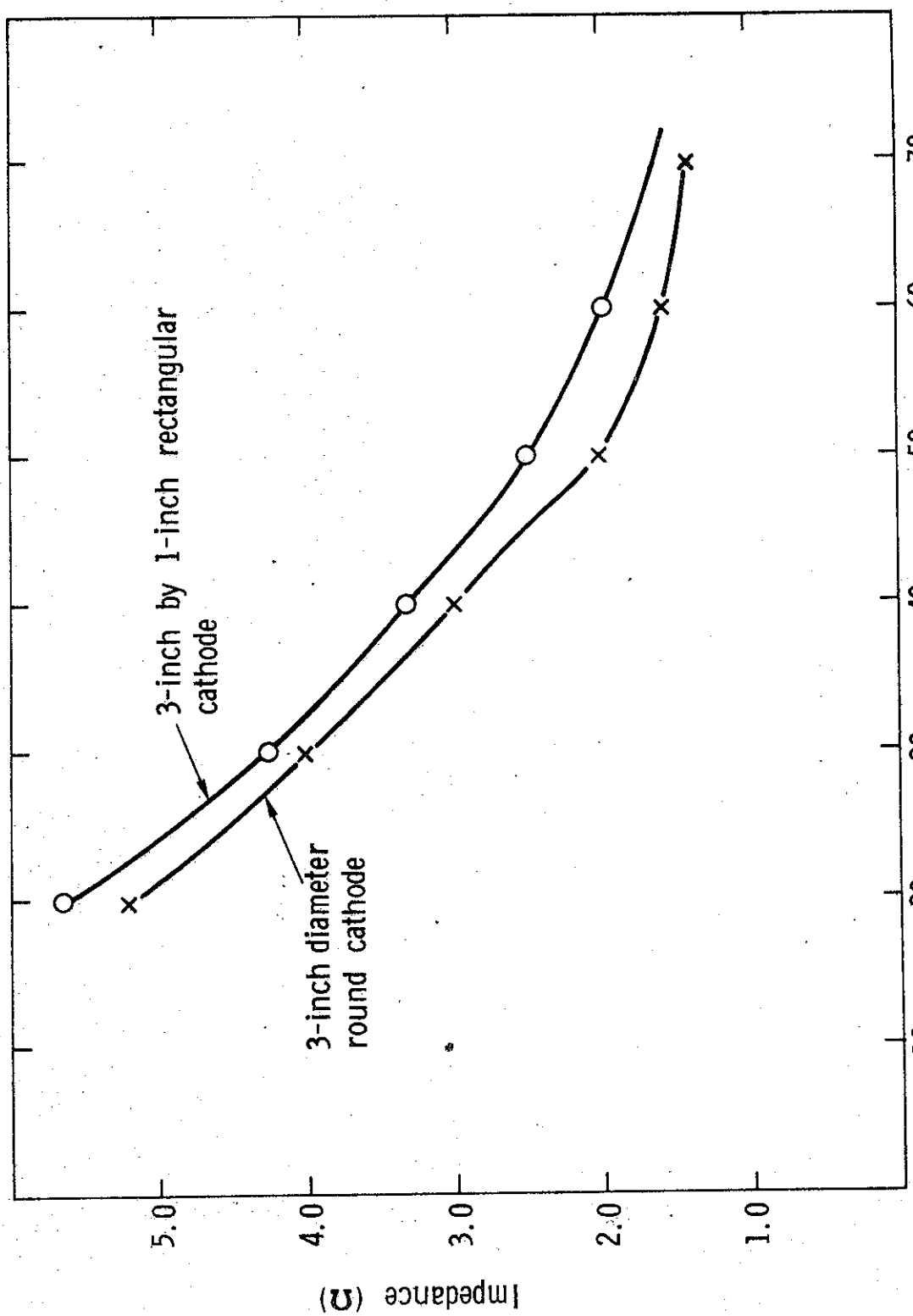

Figure 20 Impedance as a function of time for two cathodes.

SECTION 4

CONCLUSIONS

The behavior of intense beams in the diode under steady-state conditions ($dI/dt = 0$), with no externally applied magnetic fields, has been satisfactorily described by the para-potential flow model. Adjacent diodes have been magnetically decoupled in spite of large (250-kA) currents at close cathode proximity (2.86 centimeters) by extending the cathode shank within its cylindrical enclosure. Applying a B_Z field to the diode inhibits self-pinch of the beam. However, the current density is still highest at the innermost cathode radii. It is suggested that this is due to space-charge effects associated with the twisted field lines.

Propagation of intense electron beams in sufficiently conductive plasma is consistent with single-particle motion in the externally applied magnetic fields. In both linear pinch and solenoid field configurations, this effect gives high transport efficiency. The Z-pinch also allows control of beam fluence, beam combination and a degree of beam compression, while the solenoid system maintains the shape and size of the cathode over the distances that have been tested. No evidence is found for diamagnetic effects due to the beam in solenoid systems over these distances.

REFERENCES

1. G. Yonas, I. Smith, P. Spence, S. Putnam and P. Champney, "Development and Application of a 1 MV, 1 MA Mylar Dielectric Pulsed Electron Accelerator and Concepts for Higher Energy Modular Generator Systems," paper presented at Eleventh Symposium on Electron, Ion, and Laser Beam Technology, Boulder, Colorado, May 1971.

2. G. Loda and P. Spence, Bull. Am. Phys. Soc. 15:1401, 1970.

3. D. de Packh, Radiation Project Internal Report No. 7, NRL, April 1968.

4 F. Friedlander, R. Hecktel, J. Jory and C. Mosher, DASA 2173, Varian Associates, 1968.

5. J. Creedon, "A Quasi-Parapotential Model for the High ν/γ Diode," PIIR-19-70, Physics International Company, San Leandro, California, May 1970.

6. G. Yonas and P. Spence, Tenth Symposium on Electrons, Ions and Laser Beam Technology, L. Marton, editor, San Francisco Press, Inc., 1970.

7. J. Benford and B. Ecker, Bull. Am. Phys. Soc. 15:1401 and 1448, 1970.

8. J. Benford and B. Ecker, Phys. Rev. Letters, 26, 1160 (1971).

9. D. Hammer and N. Rostoker, Phys. Fluids, 13:1831, 1970.

10. C. Stallings and P. Spence, Bull. Am. Phys. Soc. 15:1401, 1970.